



HAL
open science

Effect of water chemistry on the hydro-mechanical behaviour of compacted mixtures of claystone and Na + /Ca 2+ bentonites for deep geological repositories for deep geological repositories

Zhixiong Zeng, Yu-Jun Cui, Jean Talandier

► **To cite this version:**

Zhixiong Zeng, Yu-Jun Cui, Jean Talandier. Effect of water chemistry on the hydro-mechanical behaviour of compacted mixtures of claystone and Na + /Ca 2+ bentonites for deep geological repositories for deep geological repositories. *Journal of Rock Mechanics and Geotechnical Engineering*, 2022, 14 (2), pp.527-536. 10.1016/j.jrmge.2021.09.016 . hal-04181887

HAL Id: hal-04181887

<https://enpc.hal.science/hal-04181887v1>

Submitted on 16 Aug 2023

HAL is a multi-disciplinary open access archive for the deposit and dissemination of scientific research documents, whether they are published or not. The documents may come from teaching and research institutions in France or abroad, or from public or private research centers.

L'archive ouverte pluridisciplinaire **HAL**, est destinée au dépôt et à la diffusion de documents scientifiques de niveau recherche, publiés ou non, émanant des établissements d'enseignement et de recherche français ou étrangers, des laboratoires publics ou privés.

23 **Abstract:** In the French deep geological disposal for radioactive wastes, compacted
24 bentonite/claystone mixtures have been considered as possible sealing materials. After
25 emplacement in place, such mixtures are hydrated by the site solution as well as the cement
26 solution produced by the degradation of concrete. In this study, the effects of synthetic site
27 solution and cement solution on the hydro-mechanical behaviour of compacted mixtures of
28 claystone and two types of bentonites (Na^+ MX80 and Ca^{2+} Sardinia bentonites) were investigated
29 by carrying out a series of swelling pressure, hydraulic conductivity and Mercury Intrusion
30 Porosimetry (MIP) tests. It was found that for the MX80 bentonite/claystone mixture hydrated
31 with synthetic site solution, the swelling capacity was reduced compared to the case with
32 deionised water owing to the transformation of Na-montmorillonite to multi-cation dominant
33 montmorillonite by cation exchanges. For the Sardinia bentonite/claystone mixture, the similar
34 increasing rate of swelling pressure was observed during the crystalline swelling process for
35 different solutions, suggesting insignificant cation exchanges. Additionally, the cations in the
36 synthetic site solution could reduce the thickness of diffuse double layer and the osmotic swelling
37 for both MX80 bentonite/claystone and Sardinia bentonite/claystone mixtures. The large-pore
38 volume increased consequently and enhanced water flow. In the cement solution, the hydroxide
39 could also dissolve the montmorillonite, reducing the swelling pressure, and increased the large-
40 pore volume, facilitating the water flow. Furthermore, the decrease of swelling pressure and the
41 increase of hydraulic conductivity were more significant in the case of low dry density because
42 of more intensive interaction between montmorillonite and hydroxide thanks to the high
43 permeability.

44 **Keywords:** bentonite/claystone mixture; synthetic site solution; cement solution; bentonite type;
45 swelling pressure; hydraulic conductivity

46 **1. Introduction**

47 Deep geological repository has been accepted as a solution for the long-term storage of high-level
48 radioactive wastes in many countries (Sellin and Leupin, 2013). To ensure the long-term safe isolation
49 of radioactive wastes in deep geological formations, bentonite-based materials are commonly used as
50 sealing materials (Pusch, 1982; Dixon et al., 1985; Villar and Lloret, 2008; Ye et al., 2010), while
51 cement (in mortar or concrete) is used to construct the tunnel retaining structures and tunnel
52 plugs/seals (Sánchez et al., 2006). After the repositories are closed, the bentonite-based materials will
53 be hydrated by the pore water of the host rock and swell, filling the technological voids and restricting
54 the release of radionuclides from the radioactive wastes to the surrounding environment. It has been
55 reported that the pore water of the host rock considered in several countries is of certain salinity (Deng
56 et al., 2011; Nguyen et al., 2013; Wang et al., 2014; Sun et al., 2018). In addition, the cement in
57 contact with groundwater for a long period can degrade and release a large number of Ca^{2+} and OH^- ,
58 resulting in a high-pH alkaline solution (Savage et al., 2002; Karnland et al., 2007; Anh et al., 2017;
59 Sun et al., 2018). In the performance assessment of the storage repositories, it appears essential to
60 account for the effect of such water chemistry on the hydro-mechanical behaviour of bentonite-based
61 materials.

62 In the past decades, the influence of saline solution on the hydro-mechanical behaviour of
63 bentonite-based materials was studied by many researchers (Karnland et al., 2006; Rao et al., 2006;
64 Castellanos et al., 2008; Komine et al., 2009; Zhu et al., 2013). It was found that the pore water
65 salinity could significantly decrease the swelling pressure (Komine et al., 2009; Zhu et al., 2013) and
66 increase the hydraulic conductivity (Castellanos et al., 2008; Zhu et al., 2013). Yukselen-Aksoy et al.
67 (2008) and Zhu et al. (2013) reported that the cations in the pore water might alter the mineralogical

68 compositions through cation exchanges and influence the crystalline swelling process, resulting in a
69 lower swelling pressure. Additionally, the cations in the pore water could decrease the thickness of
70 diffuse double layer, affecting the osmotic swelling behaviour ([Siddiqua et al., 2011](#); [Castellanos et
71 al., 2008](#); [Schanz and Tripathy, 2009](#); [Zhu et al., 2013](#); [Du et al., 2021](#)). At a given void ratio, a larger
72 large-pore volume could be expected for the specimen hydrated with a saline solution, leading to a
73 higher hydraulic conductivity.

74 In addition to the saline solution, alkaline solution can also significantly influence the hydro-
75 mechanical behaviour of bentonite-based materials ([Karnland et al., 2007](#); [Herbert et al., 2008](#); [Lee
76 et al., 2012](#); [Chen et al., 2016](#); [Sun et al., 2018, 2019, 2020](#); [Liu et al., 2020](#)). [Chen et al. \(2016\)](#)
77 experimentally determined the swelling pressures and hydraulic conductivities of GMZ bentonite
78 hydrated with various NaOH solutions and found that the final swelling pressure decreased and the
79 hydraulic conductivity increased significantly with the increase of NaOH solution concentration.
80 [Karnland et al. \(2007\)](#) investigated the constant-volume swelling pressures of compacted Wyoming
81 MX80 bentonite hydrated with NaOH and Ca(OH)₂ solutions and found that 0.1 M NaOH (pH=12.9)
82 or saturated Ca(OH)₂ solutions (pH=12.4) did not significantly change the swelling pressure of
83 compacted MX80 bentonite. In contrast, [Sun et al. \(2018; 2019\)](#) compared the swelling pressures and
84 mineralogical compositions of GMZ bentonite hydrated with Beishan site solution (pH=8.5), young
85 concrete water (pH=13) and evolved concrete water (pH=12) and observed a remarkably lower
86 swelling pressure in the case of young concrete water. They explained this phenomenon by the
87 dissolution of montmorillonite upon saturation with alkaline solutions and the formation of some less
88 active zeolites and calcium hydrated silicates. Additionally, the montmorillonite content decreased
89 linearly as the pH increased ([Sun et al., 2019](#)).

90 In France, Callovo-Oxfordian (COx) claystone has been considered as a potential geological
91 host rock for high-level radioactive waste disposal. To reduce the excavation waste and ensure the
92 mineralogical compatibility, a mixture of crushed COx claystone and bentonite in the form of pre-
93 compacted blocks has been proposed as a possible sealing material by the French National
94 Radioactive Waste Management Agency (Andra) (Wang et al., 2014; Zeng et al., 2019; Middelhoff,
95 2020). Wang et al. (2014) carried out a series of constant-volume swelling pressure tests on
96 compacted MX80 bentonite/COx claystone mixture with a bentonite fraction of 70% (dry density of
97 1.7 Mg/m³) and observed a slight decrease of swelling pressure with the synthetic site solution after
98 700 days of hydration. Cuisinier et al. (2009) studied the microstructure of compacted COx claystone
99 at a dry density of 1.61 Mg/m³ hydrated with portlandite-saturated solution for 1 year using mercury
100 intrusion porosimetry (MIP) and scanning electron microscopy (SEM) techniques and found an
101 increase of macro-pore void ratio after the fluid circulation. By contrast, Middelhoff (2020) indicated
102 that the swelling pressure after about 7 days and the hydraulic conductivity after 1 year were hardly
103 affected by the site solution and cement solution for the compacted MX80 bentonite/COx claystone
104 mixture (a proportion of 30/70 in dry mass) at a dry density of 1.72 Mg/m³. Up to now, there was no
105 consensus regarding the effects of site solution and cement solution on the hydro-mechanical
106 behaviour of bentonite/claystone mixture. Additionally, to the authors' knowledge, the responses of
107 the mixtures of COx claystone and different bentonites upon hydration with site solution and cement
108 solution have not been systematically studied.

109 In this study, a series of infiltration tests using deionised water, synthetic site solution and cement
110 solution were performed on compacted mixtures of COx claystone and Na⁺ MX80 and Ca²⁺ Sardinia
111 bentonites at different dry densities. The effects of synthetic site solution and cement solution on the

112 swelling pressure and hydraulic conductivity were analysed. Moreover, the microstructure features
113 before and after hydration were also determined using MIP technique, enabling the interpretation of
114 the physico-chemical interaction between different bentonite/claystone mixtures and different fluids
115 involved.

116 **2. Materials and methods**

117 *2.1. Materials*

118 According to the preliminary results of [Zeng et al. \(2020a\)](#), the bentonite/claystone mixtures with a
119 proportion of 30/70 in dry mass were used in this study to fulfill the requirements of Andra in terms
120 of swelling pressure and hydraulic conductivity with a dry density of 1.72-1.82 Mg/m³. To investigate
121 the effect of bentonite type, two bentonites, MX80 and Sardinia bentonites, were considered. The
122 MX80 bentonite is a Na-bentonite, extracted from Wyoming in the United States while the Sardinia
123 bentonite is a Ca-bentonite, taken from Monte Furros, Italy. The main physical and chemical
124 characteristics of the two bentonites are presented in [Table 1](#). The COx claystone was sampled from
125 the Andra Underground Research Laboratory (URL) in Bure. It is composed of 40–45% interstratified
126 illite/smectite, 30% carbonates, and 25%–30% quartz and feldspar. The COx claystone is
127 characterized by a liquid limit of 41%, a plastic limit of 24% and a specific gravity of 2.70. Prior to
128 testing, the bentonites and claystone were crushed to have a maximum grain size of 2.0 mm. The
129 grain size distributions of the bentonites and claystone determined by dry sieving are presented in [Fig.](#)
130 [1](#). The mean grain diameters (D_{50}) of the MX80 bentonite, Sardinia bentonite, COx claystone are 0.55,
131 1.06 and 0.58 mm, respectively.

132 Synthetic site solution and cement solution were used for the infiltration tests. These solutions
133 respectively represent the site water at a depth of 490 m and the alkaline solution after the degradation

134 of concrete, and were prepared according to the recipe provided by Andra (Table 2). The chemical
135 compositions of the solutions are summarized in Table 3. The pH values of the two solutions were
136 measured, equal to 8.6 and 12.5, respectively. In addition, deionised water was also employed as a
137 reference case.

138 2.2. Experimental methods

139 The bentonite and claystone powders with a proportion of 30/70 in dry mass were first mixed for
140 more than 10 min. The gravimetric water contents of the MX80 bentonite, Sardinia bentonite and
141 claystone under laboratory conditions (a relative humidity of about 60%) were determined by oven-
142 drying at 105-°C for 24 h, equal to 11.4, 16.0 and 6.1%, respectively. Accordingly, the respective
143 water contents of the MX80 bentonite/claystone and Sardinia bentonite/claystone mixtures were 7.7
144 and 9.1%, respectively. Based on the target dry density, a pre-determined amount of mixtures were
145 poured into a rigid steel ring with an inner diameter of 50 mm and statically compacted at a constant
146 displacement rate of 0.05 mm/min. The final height of compacted specimens was 10 mm. For the
147 MX80 bentonite/claystone mixture, nine specimens with dry densities of 1.6, 1.8 and 2.0 Mg/m³ were
148 compacted, three for each dry density (Table 4); for the Sardinia bentonite/claystone mixture, six
149 specimens with dry densities of 1.6 and 1.8 Mg/m³ were prepared. Afterwards, the compacted
150 specimens were transferred into a testing cell with an inner diameter of 50 mm (Fig. 2) and placed
151 between two porous stones and filter papers. A circular cap with a diameter of 50 mm was placed at
152 the top of the specimens and then blocked using a screw to prevent axial swelling. After that,
153 deionised water, synthetic site solution or cement solution was injected into the specimens from the
154 bottom of the cell under a water head of about 1 m and the axial swelling force was monitored using
155 a force transducer installed under the testing cell. For all the specimens, the hydration lasted for 90

156 days. All the tests were performed at constant ambient temperature (20 ± 1 °C).

157 At the end of the swelling pressure tests, the solution injection was continued for more than 24
158 h using a pressure/volume controller under constant pressures. To minimise the disturbance of the
159 microstructure and avoid hydraulic fracturing, the water injection pressure was lower than 1/10 of the
160 final swelling pressure. For the MX80 bentonite/claystone mixtures at 1.6, 1.8 and 2.0 Mg/m³ dry
161 densities, the injection pressures were respectively 0.04, 0.10 and 0.20 MPa, while those for the
162 Sardinia bentonite/claystone mixtures at 1.6 and 1.8 Mg/m³ dry densities were 0.03 and 0.10 MPa,
163 respectively. During the solution injection, the solution volume injected into the specimens was
164 recorded. After stabilization of the flow rate, the specimens were regarded as saturated and the
165 saturated hydraulic conductivity was calculated based on the Darcy's law:

$$166 \quad k = \frac{q}{iA} \quad (1)$$

167 where q is the flow rate (m³/s); i is the hydraulic gradient; A is the cross-section (m²).

168 After the infiltration tests, the specimens were taken out of the cell for microstructure
169 observation. The specimens were first cut into small pieces (about 1 cm³ in volume). Afterwards, the
170 pieces were immersed in slush nitrogen (-210°C) obtained by previously submitting it to vacuum for
171 instantaneous freezing, and then lyophilized in a vacuumed chamber (Delage et al., 1996). For the
172 MIP test, the freeze-dried pieces were put in a low pressure chamber with a working pressure from
173 3.6 to 2000 kPa and then a high pressure chamber with a working pressure from 0.2 to 228 MPa,
174 enabling identification of pore entrance diameter 350 to 0.006 μm (the diameter at the narrowest
175 position).

176 **3. Experimental results**

177 *3.1. Swelling pressure*

178 The evolutions of swelling pressure for different dry densities are depicted in Fig. 3. On the whole,
179 the curves can be divided into two stages: a relatively large primary swell (stage I) and a small
180 secondary swell (stage II). In stage I, the swelling pressure increased quickly. The overall increasing
181 rate for the MX80 bentonite/claystone mixture hydrated with synthetic site solution and cement
182 solution was slightly lower than that of the specimens hydrated with deionised water. Moreover, the
183 synthetic site and cement solutions reduced the elapsed time required to complete stage I. By contrast,
184 the increasing rate for the Sardinia bentonite/claystone mixture was almost the same regardless of the
185 permeating solutions. In stage II, for the MX80 bentonite/claystone mixture with large dry densities
186 (1.8 and 2.0 Mg/m³), the swelling pressure tended to stabilization. By contrast, for the MX80
187 bentonite/claystone mixture at a low dry density (1.6 Mg/m³) and the Sardinia bentonite/claystone
188 mixtures at dry densities of 1.6 and 1.8 Mg/m³, the swelling pressure reached a peak, decreased
189 sharply and then tended to stabilization. The specimens at a low dry density and hydrated with cement
190 solution exhibited a more remarkable decrease of swelling pressure after reaching a peak. Moreover,
191 at a given dry density, the decrease of swelling pressure after reaching a peak was more significant
192 for the Sardinia bentonite/claystone mixture compared to the MX80 bentonite/claystone mixture. The
193 final swelling pressures of the specimens at various dry densities and hydrated with different solutions
194 are summarized in Fig. 4. There were reasonable linear relationships between the final swelling
195 pressure and the dry density for the specimens hydrated with different solutions. In case of high dry
196 densities (1.8 and 2.0 Mg/m³), the final swelling pressure was almost independent of the permeating
197 solution. In case of low dry density (1.6 Mg/m³), the synthetic site solution and cement solution more
198 or less reduced the swelling pressure. Additionally, from Fig. 4, a slightly lower final swelling
199 pressure could be observed on the Sardinia bentonite/claystone mixture compared to the MX80

200 bentonite/claystone mixture, especially in the case of low dry density of 1.6 Mg/m^3 .

201 *3.2. Saturated hydraulic conductivity*

202 At the end of swelling pressures tests, the saturated hydraulic conductivities were determined for
203 various dry densities and the results are presented in [Fig. 5](#). For the specimens hydrated with a given
204 solution, the hydraulic conductivity decreased with the increase of dry density. The synthetic site
205 solution and cement solution increased the hydraulic conductivity for both the MX80
206 bentonite/claystone and the Sardinia bentonite/claystone mixtures. This is consistent with the results
207 of [Villar \(2006\)](#) and [Chen et al. \(2016\)](#) while studying the effects of saline and alkaline solutions on
208 the hydraulic conductivity of MX80 bentonite/granite mixture (a proportion of 30/70 in dry mass)
209 and GMZ bentonite, respectively. Additionally, larger increases of hydraulic conductivity due to the
210 water chemistry were observed on the specimens hydrated with cement solution. The lower the dry
211 density of specimens, the more significant the influences of synthetic site solution and cement
212 solution on the saturated hydraulic conductivity. In addition, compared to the MX80
213 bentonite/claystone mixture, the compacted Sardinia bentonite/claystone mixture exhibited a larger
214 hydraulic conductivity at the same dry density.

215 *3.3. Microstructure observation*

216 [Figs. 6 and 7](#) illustrate the pore size distributions of the specimens before and after hydration. From
217 the cumulative curves ([Figs. 6a and 7a](#)), it could be observed that the final value of intruded mercury
218 void ratio was lower than the global void ratio. This difference indicated the existence of a large
219 amount of porosity which was inaccessible with the maximum pressure applied in the MIP tests. From
220 the density curves ([Figs. 6b and 7b](#)), the as-compacted specimens exhibited a typical bimodal porosity,
221 allowing two main pore populations to be defined: a population of intra-aggregate pores (small pores)

222 with a mean pore diameter of 0.02 μm and a population of inter-aggregate pores (large pores) with
223 a mean pore diameter of 5 μm . This is consistent with the observation of Delage et al. (1996; 2006)
224 who found that the soils compacted dry of optimum could be described by a typical aggregate
225 microstructure. After hydration, the mean pore diameter of large pores increased to about 25 μm . By
226 contrast, the mean pore diameter of small pores remained unchanged but the peak value decreased
227 remarkably. For the specimens at low dry densities (1.6 and 1.8 Mg/m^3), a new pore population with
228 a mean diameter of 0.2-0.5 μm (defined as medium pores) appeared between the large and small
229 pores. Following the suggestion of [Bian et al. \(2019\)](#) and [Zeng et al. \(2020b\)](#), the respective delimiting
230 diameters between the large and medium pores and between the medium and small pore were taken
231 as 2 and 0.04 μm , respectively. To further investigate the effects of synthetic site solution and cement
232 solution on the pore structure of bentonite/claystone mixtures, the void ratios of four populations were
233 determined based on the delimiting values and the cumulative curves. The results are summarized in
234 [Figs. 8 and 9](#). It can be clearly observed that the synthetic site solution and cement solution increased
235 the larger-pore and small-pore void ratios and decreased the medium-pore void ratio. Similar
236 phenomenon was observed by [Wang et al. \(2014\)](#) and [Liu et al. \(2020\)](#) while investigating the effect
237 of saline solution on the pores structure of compacted MX80 bentonite/claystone (70/30 in dry mass)
238 and the effect of NaOH solution on the pore structure of compacted GMZ bentonite, respectively.
239 Moreover, the cement solution had a more remarkable influence on the pore structure changes than
240 the synthetic site solution. Comparison of the pore structures of two bentonite/claystone mixtures
241 shows that at a given dry density, the Sardinia bentonite/claystone mixture exhibited a lower large-
242 pore void ratio and larger medium-pore and small-pore void ratios than the MX80 bentonite/claystone
243 mixture.

244 **4. Interpretation and discussion**

245 *4.1. Effects of synthetic site solution and cement solution on hydro-mechanical behaviour*

246 When the clay minerals in the bentonite/claystone mixtures were wetted with water, their hydration
247 could be described by crystalline and osmotic swelling processes (Mitchell, 1993). At a low relative
248 humidity, crystalline hydration is the predominant mechanism with water molecules being
249 progressively adsorbed on the clay surfaces layer by layer, leading to an increase of the intra-
250 aggregate pore volume. Meanwhile, the swollen aggregates invaded the inter-aggregate pores and
251 reduced the inter-aggregate-pore volume. Obviously, this process depended on the global dry density.
252 The lower the dry density, the more significant the swelling of aggregates. With the transformation
253 of intra-aggregate and inter-aggregate pores to the medium-pore population, a remarkable increase of
254 medium-pore void ratio occurred (Figs. 8 and 9). During the crystalline swelling process, the clay
255 particles would be divided into smaller ones and fissure-like 2-dimensional (2-D) pores with a mean
256 pore size of 20 μm appeared. The variation of large-pore volume after hydration was due to the
257 combined effects of the invasion of swollen clay particles and the appearance of 2-D pores. As the
258 suction decreased down to 4 MPa, the crystalline swelling reached a nearly steady state and a
259 significant amount of water would be stored in inter-particle pores (Saiyouri et al., 2000). Due to the
260 difference of cation concentration between the pore water and the clay particle surface, diffuse double
261 layer would develop on a parallel assembly of clay particles (Liu, 2013) and osmotic swelling took
262 place.

263 Generally, the maximum number of water molecule layers intercalated between the unit layers
264 depends on the clay type and the available cations in the permeating water (Marcial et al., 2002; Liu,
265 2013). If the cation in the pore water is characterized by a high replacing power, cation exchanges
266 can take place and the clay type will change. A typically competitive order that has been commonly

267 admitted is: $\text{Na}^+ < \text{K}^+ < \text{Mg}^{2+} < \text{Ca}^{2+}$ (Mitchell, 1993; Mata, 2003; Sun et al., 2018). As shown in Table
268 3, the synthetic site solution and cement solution used in this study contain a certain amount of K^+ ,
269 Mg^{2+} or Ca^{2+} cations. According to the X-Ray diffractometry (XRD) results on GMZ bentonite by
270 Sun et al. (2019), Na-montmorillonite would be transformed to Mg/Ca- dominant montmorillonite
271 and Ca- dominant montmorillonite after the interaction with synthetic site solution and cement
272 solution, respectively. During the crystalline swelling process, the water adsorption capacity of Na-
273 montmorillonite was larger than that for Ca-montmorillonite (Liu, 2013; Du et al., 2020; Yotsuji et
274 al., 2021). Therefore, this transformation of Na-montmorillonite would decrease the swelling capacity
275 of the montmorillonite. Additionally, as the cation concentration of pore water increased, the repulsive
276 force between the diffuse double layer and the thickness of the diffuse double layer decreased (Yong
277 and Warkentin, 1975; Mitchell, 1976). Consequently, a lower swelling pressure was observed for the
278 specimens hydrated with synthetic site solution (Fig. 4). At a given global void ratio, this decreased
279 distance between clay particles leads to an increase of the large-pore void ratio. As a result, a larger
280 hydraulic conductivity was observed for the specimens hydrated with synthetic site solution (Fig. 5)
281 (Cuisinier et al., 2011).

282 Apart from the cations, the hydroxide in the cement solution can also greatly influence the hydro-
283 mechanical behaviour of the bentonite/claystone mixtures. Upon contact with hydroxide, the
284 montmorillonite might be dissolved, forming secondary minerals with much lower swelling capacity,
285 such as analcime and calcium hydrated silicates gels (Sun et al., 2018; 2019). As result, the swelling
286 capacity was reduced (Fig. 4). The produced calcium hydrated silicates gels were characterized by a
287 large amount of small pores (Wang et al., 2017), leading to an increase of small-pore void ratio of the
288 specimens hydrated with cement solution (Figs. 8 and 9) (Sun et al., 2019; Liu et al., 2020). By

289 contrast, the dissolution of montmorillonite would lead to an increase of the large-pore volume (Chen
290 et al., 2016). Compared to the specimens hydrated with synthetic site solution, the specimens could
291 be affected by the hydroxide in addition to the cations. Thus, the specimens hydrated with cement
292 solution exhibited a larger large-pore volume and a higher hydraulic conductivity compared with
293 those hydrated with synthetic site solution (Fig. 5).

294 *4.2. Effects of bentonite type and dry density on hydro-mechanical behaviour*

295 Basically, the synthetic site solution and cement solution can influence the hydro-mechanical
296 behaviour of bentonite-based materials mainly by means of cation exchanges, osmotic effect and
297 montmorillonite dissolution. After the MX80 bentonite/claystone and Sardinia bentonite/claystone
298 mixtures were in contact with synthetic site solution, cation exchanges could occur in the MX80
299 bentonite/claystone mixture, with the transformation of some Na-montmorillonite to Mg-, and Ca-
300 montmorillonite, while the Sardinia bentonite/claystone mixture would be immune to the cation
301 exchange. This would reduce the swelling capacity of MX80 bentonite/claystone mixture. Thus, a
302 slightly smaller increasing rate of swelling pressure for this mixture in stage I for MX80
303 bentonite/claystone mixture, as compared to that hydrated with deionised water (Fig. 3a and b).
304 Thanks to the higher permeability, the interaction between clay minerals and solution became more
305 intensive for the MX80 bentonite/claystone mixture at a lower dry density upon the hydration with
306 the synthetic site solution. By contrast, the cations in the synthetic site solution would exert an
307 influence on the osmotic swelling of both the MX80 bentonite/claystone and the Sardinia
308 bentonite/claystone mixtures at low dry densities. In general, the clay particles of Na-montmorillonite
309 after crystalline swelling are thinner than those of Ca-montmorillonite (Saiyouri et al., 2004). It was
310 reported that the clay particles are composed of 2–20 (and even more) aligned unit layers in Ca-

311 montmorillonite, but only of 1–5 unit layers in Na-montmorillonite (Liu, 2013). Therefore, during the
312 osmotic swelling process, few double layer development could be expected in the Ca-montmorillonite,
313 as compared to the Na-montmorillonite. The weaker osmotic swelling of Sardinia bentonite/claystone
314 mixture could not compensate the reduction of swelling pressure induced by the collapse of aggregate
315 structure. Thus, a more significant decrease was observed in stage II at low dry densities (Fig. 3a and
316 b). Additionally, the cations in the synthetic site solution could reduce the repulsive force and the
317 thickness of diffuse double layer, resulting in a lower swelling pressure and a higher hydraulic
318 conductivity for the specimens hydrated with synthetic site solution (Figs. 4 and 5). For the specimens
319 at high dry densities, the low amount of inter-particle water was insufficient to form the diffuse double
320 layer (Pusch and Yong, 2006) and the effect of cations on the swelling pressure and hydraulic
321 conductivity of the highly compacted MX80 bentonite/claystone and Sardinia bentonite/claystone
322 mixtures was less significant.

323 **5. Conclusions**

324 The effects of synthetic site solution and cement solution on the hydro-mechanical behaviour of
325 compacted Na⁺ MX80 bentonite/claystone and Ca²⁺ Sardinia bentonite/claystone mixtures were
326 investigated by carrying out a series of swelling pressure and hydraulic conductivity tests together
327 with microstructure observation. The results obtained allow the following conclusions to be drawn:

328 For the MX80 bentonite/claystone mixture, the cations in synthetic site solution could transform
329 the Na-montmorillonite to multi-cation dominant montmorillonite, reducing the swelling capacity
330 of the mixture. By contrast, for the Sardinia bentonite/claystone mixture, the cations in synthetic site
331 solution did not significantly change the Ca-montmorillonite during the crystalline swelling. Thus,
332 an insignificant effect was identified on the swelling pressure.

333 During the osmotic swelling, the presence of cations reduced the repulsive force by diffuse
334 double layer and thus swelling pressure for both the MX80 bentonite/claystone and Sardinia
335 bentonite/claystone mixtures. Additionally, a smaller thickness of diffuse double layer and a greater
336 large-pore volume could be expected for the specimens hydrated with synthetic site solution. Thus, a
337 slightly higher saturated hydraulic conductivity was obtained in that case, as compared to the case of
338 deionised water. Furthermore, a more significant influence of synthetic site solution was observed on
339 the specimens at a lower dry density thanks to the well-developed diffuse double layer.

340 In addition to the cations, the hydroxide also reduced the swelling pressure of both the MX80
341 bentonite/claystone and Sardinia bentonite/claystone mixtures. The hydroxide led to a slight increase
342 of large-pore volume and thus an increase of saturated hydraulic conductivity. Moreover, the lower
343 the dry density, the more intensive the interaction between the montmorillonite and hydroxide and
344 the more significant the changes in swelling pressure and hydraulic conductivity, due to the higher
345 permeability.

346 Over the experiment time scale of 90 days, only a slight deterioration of sealing performance of
347 the bentonite/claystone mixture was identified due to the low cation concentration and the low ionic
348 strength of permeating solutions. The effect of water chemistry in the very long-term lifespan of the
349 underground radioactive waste repository needs to be investigated in further work.

350

351 **Acknowledgments**

352 The research work was supported by Ecole des Ponts ParisTech and the French National Radioactive
353 Waste Management Agency (Andra). The first author is grateful to the China Scholarship Council
354 for the grant scholarship.

355 **References**

- 356 Anh, H.N., Ahn, H., Jo, H.Y., Kim, G.Y., 2017. Effect of alkaline solutions on bentonite properties.
357 Environmental Earth Sciences, 76(10), 374.
- 358 Bian, X., Cui, Y.J., Li, X.Z., 2019. Voids effect on the swelling behaviour of compacted bentonite.
359 Géotechnique, 69(7), 593-605.
- 360 Cara, S., Carcangiu, G., Padalino, G., Palomba, M., Tamanini, M., 2000. The bentonites in
361 pelotherapy: chemical, mineralogical and technological properties of materials from Sardinia
362 deposits (Italy). Applied Clay Science, 16(1-2), 117-124.
- 363 Castellanos, E., Villar, M.V., Romero, E., Lloret, A., Gens, A., 2008. Chemical impact on the hydro-
364 mechanical behaviour of high-density FEBEX bentonite. Physics and Chemistry of the Earth,
365 Parts A/B/C 33, S516-S526.
- 366 Chen, B., Guo, J.X., Zhang, H.X., 2016. Alteration of compacted GMZ bentonite by infiltration of
367 alkaline solution. Clay Minerals, 51(2), 237-247.
- 368 Cuisinier, O., Deneele, D., Masrouri, F., 2009. Shear strength behaviour of compacted clayey soils
369 percolated with an alkaline solution. Engineering geology, 108(3-4), 177-188.
- 370 Cuisinier, O., Auriol, J.C., Le Borgne, T., Deneele, D., 2011. Microstructure and hydraulic
371 conductivity of a compacted lime-treated soil. Engineering geology, 123(3), 187-193.
- 372 Delage, P., Audiguier, M., Cui, Y.J., Howat, M.D., 1996. Microstructure of a compacted silt.
373 Canadian Geotechnical Journal, 33(1), 150-158.
- 374 Delage, P., Marcial, D., Cui, Y.J., Ruiz, X., 2006. Ageing effects in a compacted bentonite: a
375 microstructure approach. Géotechnique, 56(5), 291-304.
- 376 Deng, Y.F., Tang, A.M., Cui, Y.J., Nguyen, X.P., Li, X.L., Wouters, L., 2011. Laboratory hydro-

377 mechanical characterisation of Boom Clay at Essen and Mol. *Physics and Chemistry of the Earth,*
378 *Parts A/B/C*, 36(17-18), 1878-1890.

379 Dixon, D.A., Gray, M.N., Thomas, A.W., 1985. A study of the compaction properties of potential
380 clay-sand buffer mixtures for use in nuclear fuel waste disposal. *Eng. Geol.* 21(3/4): 247-255.

381 Du, J.P., Zhou, A.N., Lin, X., Bu, Y., Kodikara, J., 2020. Revealing expansion mechanism of cement-
382 stabilized expansive soil with different interlayer cations through molecular dynamics
383 simulations. *The Journal of Physical Chemistry C*, 124(27), 14672-14684.

384 Du, J.P., Zhou, A.N., Lin, X., Bu, Y., Kodikara, J., 2021. Prediction of swelling pressure of expansive
385 soil using an improved molecular dynamics approach combining diffuse double layer theory.
386 *Applied Clay Science*, 203, 105998.

387 Heikola, T., Kumpulainen, S., Vuorinen, U., Kiviranta, L., Korkeakoski, P., 2013. Influence of
388 alkaline (pH 8.3–12.0) and saline solutions on chemical, mineralogical and physical properties
389 of two different bentonites. *Clay Minerals*, 48(2), 309-329.

390 Herbert, H., Kasbohm, J., Sprenger, H., Fernández, A.M., Reichelt, C., 2008. Swelling pressures of
391 MX-80 bentonite in solutions of different ionic strength. *Phys. Chem. Earth*, 33, S327–S342.

392 Karnland, O., Olsson, S., Nilsson, U., 2006. Mineralogy and sealing properties of various bentonites
393 and smectite-rich clay materials. Technical Report No. TR-06-30. SKB, Swedish Nuclear Fuel
394 and Waste Management Co.

395 Karnland, O., Olsson, S., Nilsson, U., Sellin, P., 2007. Experimentally determined swelling pressures
396 and geochemical interactions of compacted Wyoming bentonite with highly alkaline solutions.
397 *Phys. Chem. Earth*, 32(1–7), 275–286.

398 Komine, H., Yasuhara, K., Murakami, S., 2009. Swelling characteristics of bentonites in artificial

399 seawater. *Can. Geotech. J.*, 46, 177–189.

400 Lee, J.O., Lim, J.G., Kang, I.M., Kwon, S., 2012. Swelling pressures of compacted Cabentonite. *Eng.*
401 *Geol.* 129-130, 20–26.

402 Liu, L., 2013. Prediction of swelling pressures of different types of bentonite in dilute solutions.
403 *Colloids and Surfaces A: Physicochemical and Engineering Aspects*, 434, 303-318.

404 Liu, L.N., Chen, Y.G., Ye, W.M., Cui, Y.J., Wu, D.B., 2020. Swelling pressure deterioration of
405 compacted GMZ bentonite and its structural damage under heat combined with hyperalkaline
406 conditions. *Geomechanics and Geoengineering*, 1-12.

407 Mata, C., 2003. Hydraulic behaviour of bentonite based mixtures in engineered barriers: the Backfill
408 and Plug Test at the Åspö HRL (Sweden). (Ph.D. Thesis) Universitat Politècnica de Catalunya,
409 Barcelona (257 pp.).

410 Marcial, D., Delage, P., Cui, Y.J., 2002. On the high stress compression of bentonites. *Canadian*
411 *Geotechnical Journal*, 39(4), 812-820.

412 Mitchell, J.K., 1976. *Fundamentals of Soil Behaviour*. 1st edition. J. Wiley and Sons Publishers,
413 Toronto.

414 Mitchell, J.K., 1993. *Fundamentals of soil behaviour*, 2nd edn. John Wiley and sons, New York.

415 Middelhoff, M., 2020. Hydro-mechanical behavior of claystone-based backfill materials under geo-
416 environmental conditions. PhD thesis, Université de lorraine.

417 Nguyen, X.P., Cui, Y.J., Tang, A.M., Deng, Y.F., Li, X.L., Wouters, L., 2013. Effects of pore water
418 chemical composition on the hydro-mechanical behavior of natural stiff clays. *Engineering*
419 *geology*, 166, 52-64.

420 Pusch, R., 1982. Mineral–water interactions and their influence on the physical behavior of highly

421 compacted Na bentonite. Canadian Geotechnical Journal, 19(3): 381-387.

422 Pusch, R., Karnland, O., 1988. Geological evidence of smectite longevity: The Sardinian and Gotland
423 cases. Svensk kärnbränslehantering.

424 Pusch, R., Yong, R.N., 2006. Microstructure of smectite clays and engineering performance. CRC
425 Press.

426 Rao, S.M., Thyagaraj, T., Thomas, H.R., 2006. Swelling of compacted clay under osmotic gradients.
427 Géotechnique, 56(10), 707–713.

428 Saiyouri, N., Hicher, P.Y., Tessier, D., 2000. Microstructural approach and transfer water modelling
429 in highly compacted unsaturated swelling clays. Mechanics of Cohesive - frictional Materials:
430 An International Journal on Experiments, Modelling and Computation of Materials and
431 Structures, 5(1), 41-60.

432 Saiyouri, N., Tessier, D., Hicher, P.Y., 2004. Experimental study of swelling in unsaturated
433 compacted clays. Clay minerals, 39(4), 469-479.

434 Sánchez, L., Cuevas, J., Ramírez, S., De León, D.R., Fernández, R., Villa, R.V.D., Leguey, S., 2006.
435 Reaction kinetics of FEBEX bentonite in hyperalkaline conditions resembling the cement–
436 bentonite interface. Applied Clay Science, 33(2), 125-141.

437 Savage, D., Noy, D., Mihara, M., 2002. Modelling the interaction of bentonite with hyperalkaline
438 fluids. Appl. Geochem. 17, 207–223.

439 Schanz, T., Tripathy, S., 2009. Swelling pressure of a divalent - rich bentonite: Diffuse double -
440 layer theory revisited. Water Resources Research, 45(5).

441 Sellin, P. Leupin, O.X., 2013. The use of clay as an engineered barrier in radioactive-waste
442 management—a review. Clays and Clay Minerals, 61(6), 477-498.

443 Siddiqua S, Blatz, J., Siemens, G., 2011. Evaluation of the impact of pore fluid chemistry on the
444 hydromechanical behavior of claybased sealing materials. *Can Geotechn J*, 48, 199–213.

445 Sun, Z., Chen, Y.G., Cui, Y.J., Xu, H.D., Ye, W.M., Wu, D.B., 2018. Effect of synthetic water and
446 cement solutions on the swelling pressure of compacted Gaomiaozi (GMZ) bentonite: the
447 Beishan site case, Gansu, China. *Engineering Geology*, 244, 66-74.

448 Sun, Z., Chen, Y.G., Cui, Y.J., Ye, W.M., Chen, B., 2019. Effect of synthetic Beishan site water and
449 cement solutions on the mineralogy and microstructure of compacted Gaomiaozi (GMZ)
450 bentonite. *Soils and Foundations*, 59 (6), 2056-2069.

451 Sun, Z., Chen, Y.G., Ye, W.M., Cui, Y.J., Wang, Q., 2020. Swelling deformation of Gaomiaozi
452 bentonite under alkaline chemical conditions in a repository. *Engineering Geology*, 279, 105891.

453 Villar, M.V., 2006. Infiltration tests on a granite/bentonite mixture: Influence of water salinity.
454 *Applied Clay Science*, 31(1-2), 96-109.

455 Villar, M.V., Lloret, A. 2008. Influence of dry density and water content on the swelling of a
456 compacted bentonite. *Appl. Clay Sci.* 39(1–2), 38–49.

457 Vitale, E., Deneele, D., Russo, G., 2016. Multiscale analysis on the behaviour of a lime treated
458 bentonite. *Procedia Engineering*, 158, 87-91.

459 Wang, Q., Cui, Y.J., Tang, A.M., Delage, P., Gatmiri, B., Ye, W.M., 2014. Long-term effect of water
460 chemistry on the swelling pressure of a bentonite-based material. *Applied clay science*, 87, 157-
461 162.

462 Wang, Y., Duc, M., Cui, Y.J., Tang, A.M., Benahmed, N., Sun, W.J., Ye, W.M., 2017. Aggregate
463 size effect on the development of cementitious compounds in a lime-treated soil during curing.
464 *Applied Clay Science*, 136, 58-66.

465 Ye, W.M., Chen, Y.G., Chen, B., Wang, Q., Wang, J., 2010. Advances on the knowledge of the
466 buffer/backfill properties of heavily-compacted GMZ bentonite. *Engineering Geology*, 116(1-
467 2), 12-20.

468 Yong, R.N., Warkentin, B.P., 1975. *Soil Properties and Behaviour*. Elsevier, Amsterdam.

469 Yotsuji, K., Tachi, Y., Sakuma, H., Kawamura, K., 2021. Effect of interlayer cations on
470 montmorillonite swelling: Comparison between molecular dynamic simulations and
471 experiments. *Applied Clay Science*, 204, 106034.

472 Yukselen-Aksoy, Y., Kaya, A., Ören, A.H., 2008. Seawater effect on consistency limits and
473 compressibility characteristics of clays. *Eng. Geol.*, 102, 54–61.

474 Zeng, Z.X., Cui, Y.J., Zhang, F., Conil, N., Talandier, J., 2019. Investigation of swelling pressure of
475 bentonite/claystone mixture in the full range of bentonite fraction. *Applied Clay Science*.

476 Zeng, Z., Cui, Y. J., Conil, N., Talandier, J., 2020a. Experimental Investigation and Modeling of the
477 Hydraulic Conductivity of Saturated Bentonite–Claystone Mixture. *International Journal of*
478 *Geomechanics*, 20(10), 04020184.

479 Zeng, Z., Cui, Y.J., Conil, N., Talandier, J., 2020b. Effects of technological voids and hydration time
480 on the hydro-mechanical behaviour of compacted bentonite/claystone mixture. *G éotechnique*, 1-
481 14.

482 Zhu, C.M., Ye, W.M., Chen, Y.G., Chen, B., Cui, Y.J., 2013. Influence of salt solutions on the
483 swelling pressure and hydraulic conductivity of compacted GMZ01 bentonite. *Eng. Geol.*, 166,
484 74–80.

485 **List of Tables**

486 Table 1 Physical and chemical properties of MX80 and Sardinia bentonites

487 Table 2 Recipe for the synthetic site solution and cement solution preparation

488 Table 3 Composition of the synthetic site solution and cement solution

489 Table 4 Experimental programme

490 **List of Figures**

491 Fig. 1 Grain size distribution of MX80 and Sardinia bentonites and crushed COx claystone

492 Fig. 2 Schematic diagram of the constant-volume cell for swelling pressure and hydraulic
493 conductivity tests

494 Fig. 3 Evolution of axial swelling pressure of specimens at different dry densities. (a) 1.6 Mg/m³, (b)
495 1.8 Mg/m³ and (c) 2.0 Mg/m³

496 Fig. 4 Final swelling pressure versus dry density

497 Fig. 5 Hydraulic conductivity versus dry density

498 Fig. 6 Pore size distribution of MX80 bentonite/claystone mixtures: (a) cumulative curves of
499 specimens at a dry density of 1.6 Mg/m³, (b) density function curves of specimens with a dry density
500 of 1.6 Mg/m³, (c) cumulative curves of specimens at a dry density of 1.8 Mg/m³, (d) density function
501 curves of specimens at a dry density of 1.8 Mg/m³, (e) cumulative curves of specimens at a dry density
502 of 2.0 Mg/m³ and (f) density function curves of specimens at a dry density of 2.0 Mg/m³

503 Fig. 7 Pore size distribution of Sardinia bentonite/claystone mixtures: (a) cumulative curves of
504 specimens at a dry density of 1.6 Mg/m³, (b) density function curves of specimens at a dry density of
505 1.6 Mg/m³, (c) cumulative curves of specimens at a dry density of 1.8 Mg/m³ and (d) density function
506 curves of specimens at a dry density of 1.8 Mg/m³

507 Fig. 8 Changes in inaccessible-pore, small-pore, medium-pore and large-pore void ratios for the
508 compacted MX80 bentonite/claystone mixtures. (a) 1.6 Mg/m³, (b) 1.8 Mg/m³ and (c) 2.0 Mg/m³

509 Fig. 9 Changes in inaccessible-pore, small-pore, medium-pore and large-pore void ratios for the
510 compacted Sardinia bentonite/claystone mixtures. (a) 1.6 Mg/m³ and (b) 1.8 Mg/m³

511 **Table 1** Physical and chemical properties of MX80 and Sardinia bentonites

Soil property	MX80	Sardinia
Specific gravity	2.76	2.54 ^b
Consistency limit		
Liquid limit (%)	494	143 ^b
Plastic limit (%)	46	69 ^b
Plasticity index (%)	448	74 ^b
Cation exchange capacity (CEC) (meq/100 g)	80 ^a	65 ^c
Main minerals	Montmorillonite (86%) Quartz (7%)	Montmorillonite (60-90%) ^d Illite (10-14%) ^d

512 a Karnland et al. (2006)

513 b Vitale et al. (2016)

514 c Cara et al. (2000)

515 d Pusch and Karnland (1988)

516

Table 2 Recipe for the synthetic site solution and cement solution preparation

Content (g/L)	NaCl	NaHCO ₃	KCl	CaSO ₄ •2H ₂ O	MgSO ₄ •7H ₂ O	CaCl ₂ •2H ₂ O	Na ₂ SO ₄	Ca(OH) ₂
Site solution	1.950	0.130	0.035	0.630	1.020	0.080	0.700	-
Cement solution	1.286	-	0.596	-	-	-	-	1.408

517

518 **Table 3** Composition of the synthetic site solution and cement solution

Compound (mmol/L)	Na ⁺	K ⁺	Ca ²⁺	Mg ²⁺	Cl ⁻	SO ₄ ²⁻	CO ₃ ²⁻
Site solution	44.6	0.47	4.2	4.1	34.8	12.7	1.58
Cement solution	22.2	8.05	19	-	30.2	-	-

519

Table 4 Experimental programme

Test No.	Bentonite type	Dry density (Mg/m ³)	Injected water	MIP
T01	MX80	1.6	Deionised water	✓
T02	MX80	1.6	Site solution	✓
T03	MX80	1.6	Cement solution	✓
T04	MX80	1.8	Deionised water	✓
T05	MX80	1.8	Site solution	✓
T06	MX80	1.8	Cement solution	✓
T04	MX80	2.0	Deionised water	✓
T05	MX80	2.0	Site solution	✓
T06	MX80	2.0	Cement solution	✓
T04	Sardinia	1.6	Deionised water	✓
T05	Sardinia	1.6	Site solution	✓
T06	Sardinia	1.6	Cement solution	✓
T04	Sardinia	1.8	Deionised water	✓
T05	Sardinia	1.8	Site solution	✓
T06	Sardinia	1.8	Cement solution	✓

522
523

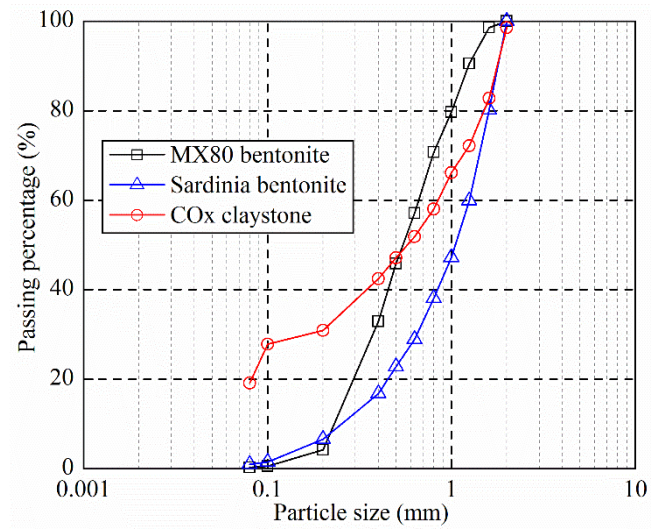


Fig. 1 Grain size distribution of MX80 and Sardinia bentonites and crushed COx claystone

524
525

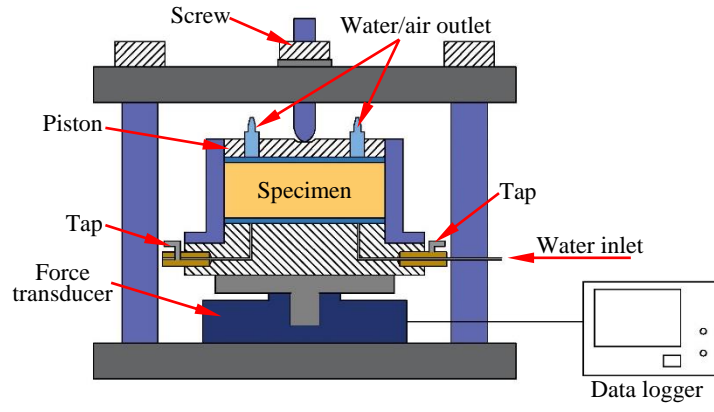
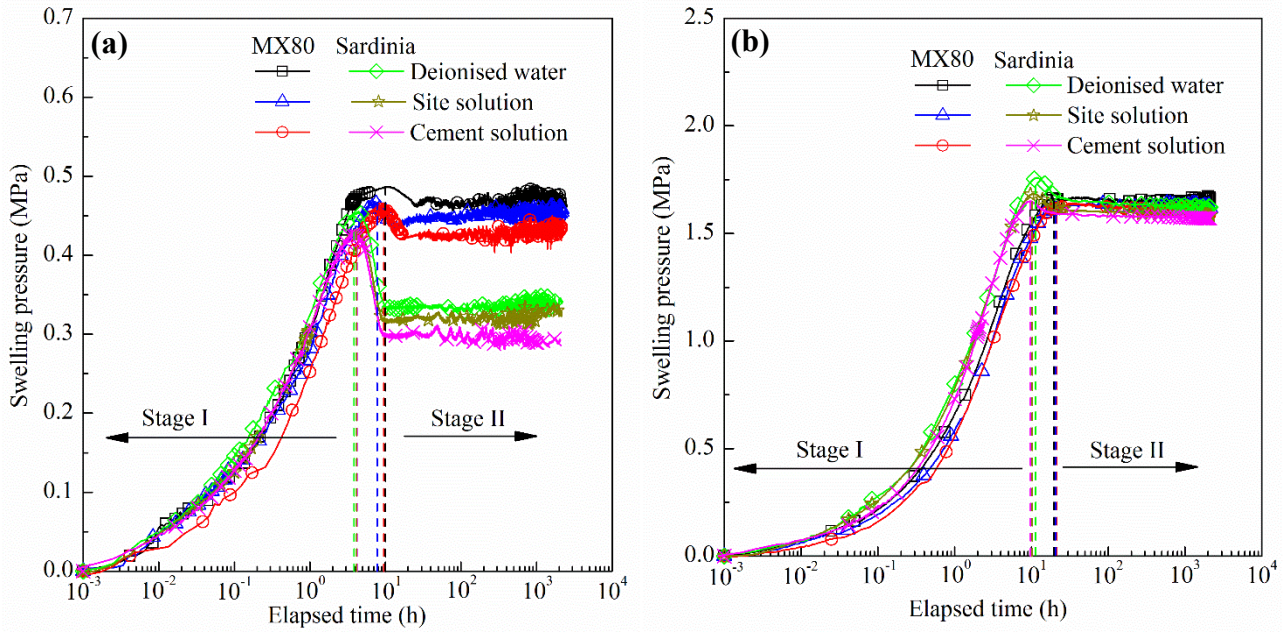


Fig. 2 Schematic diagram of the constant-volume cell for swelling pressure and hydraulic conductivity tests

526



527

528

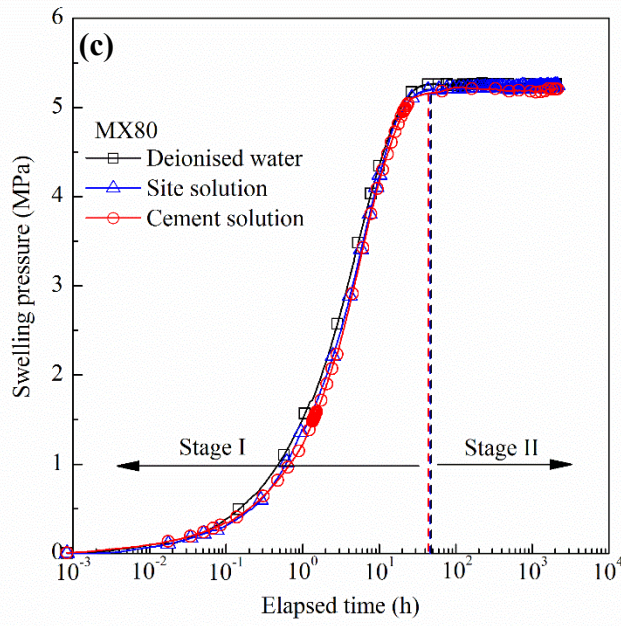


Fig. 3 Evolution of axial swelling pressure of specimens at different dry densities. (a) 1.6 Mg/m³, (b) 1.8 Mg/m³ and (c) 2.0 Mg/m³

529
530

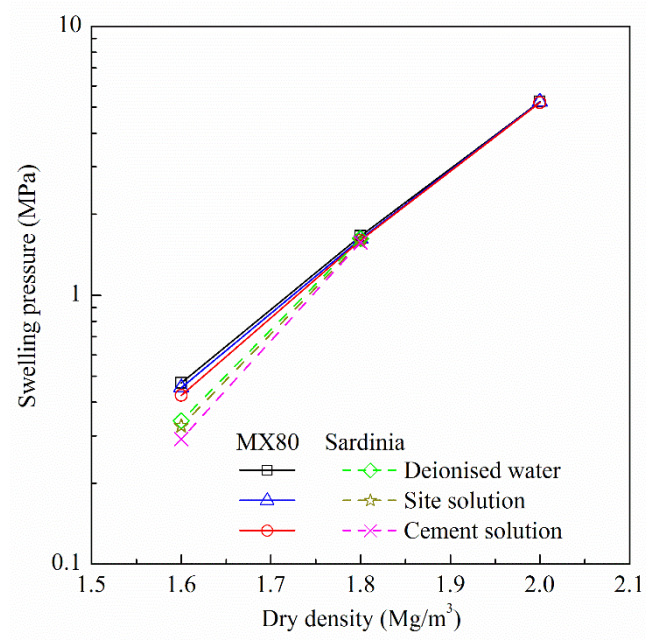


Fig. 4 Final swelling pressure versus dry density

531
532

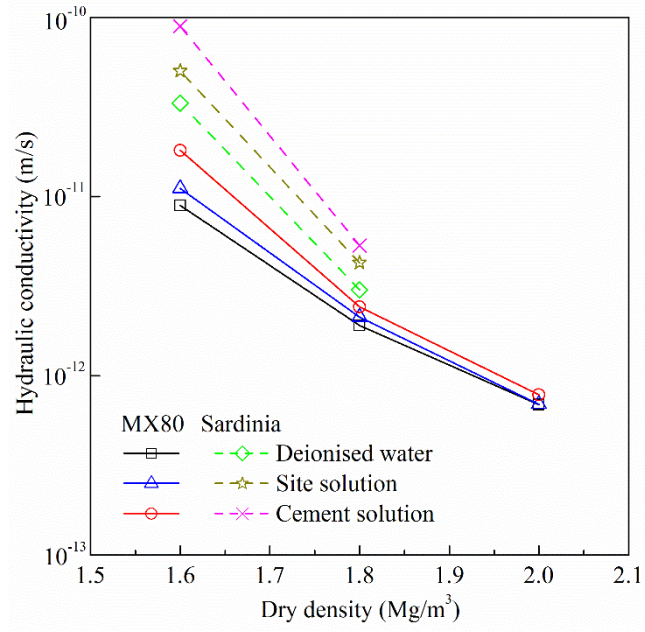
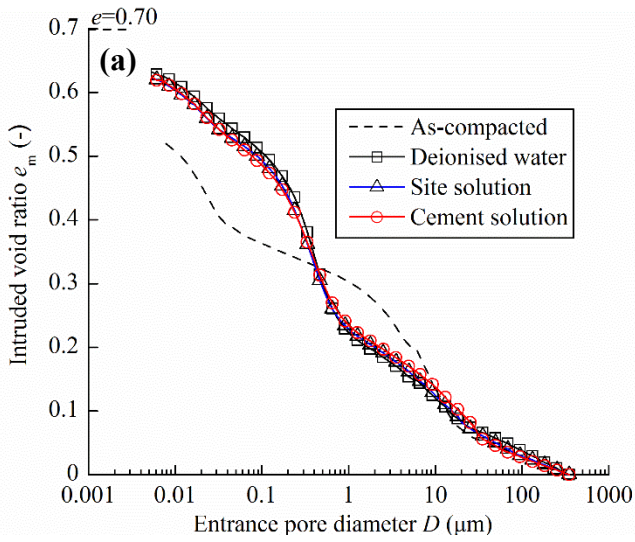
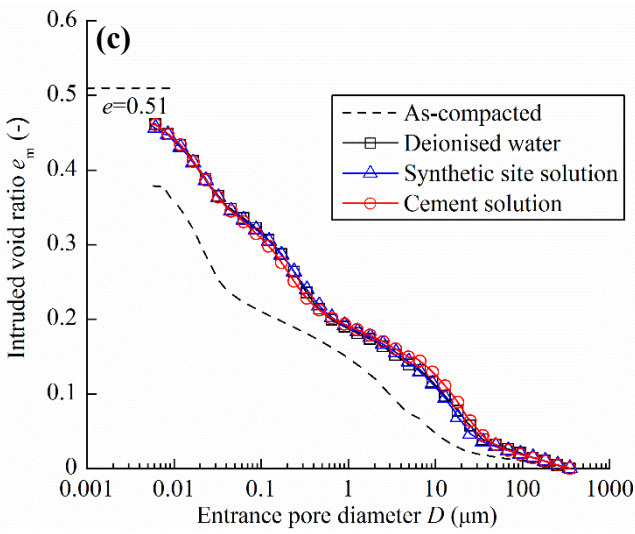
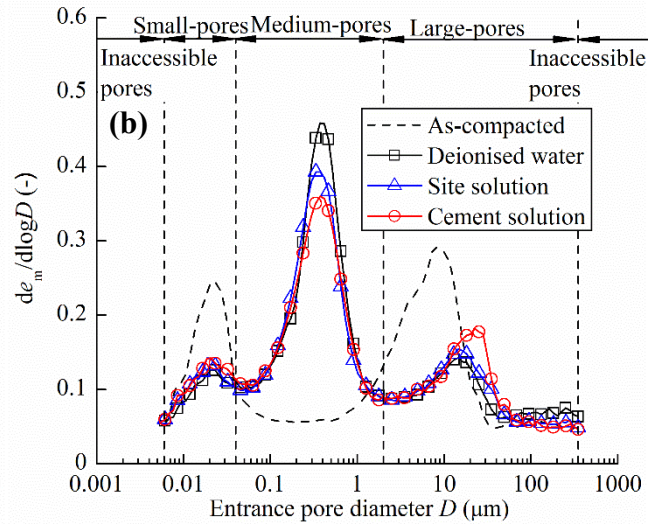


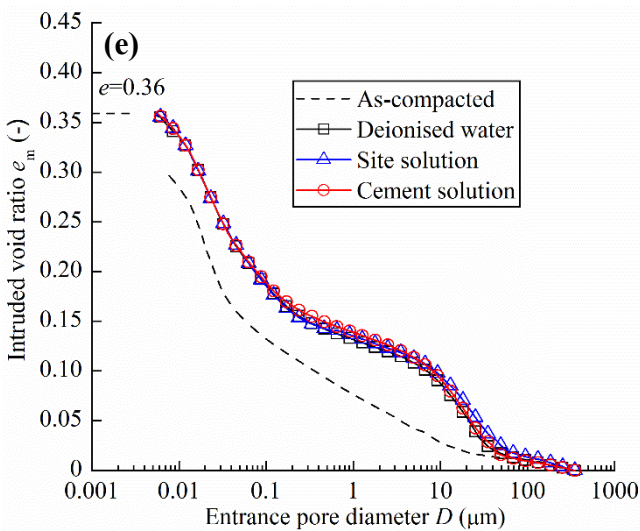
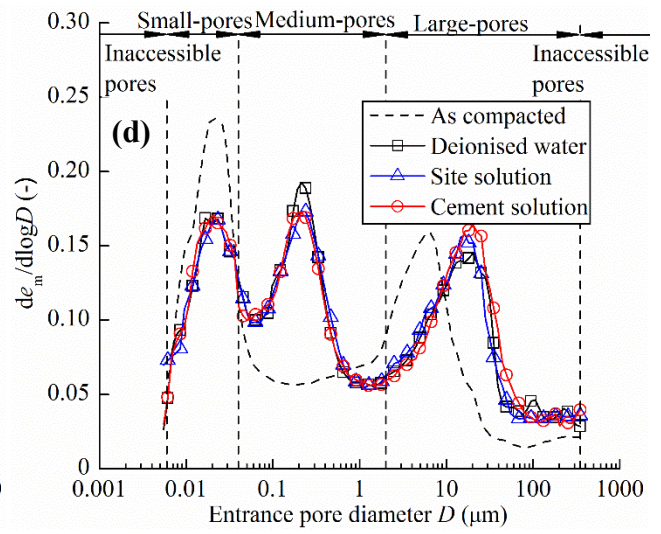
Fig. 5 Hydraulic conductivity versus dry density



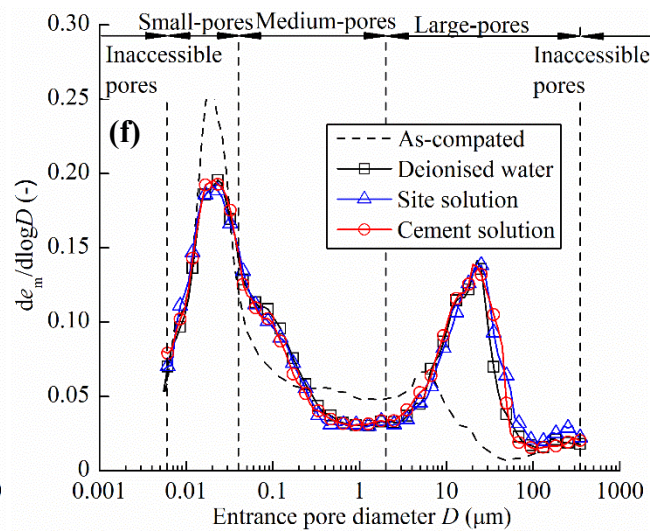
533



534



535



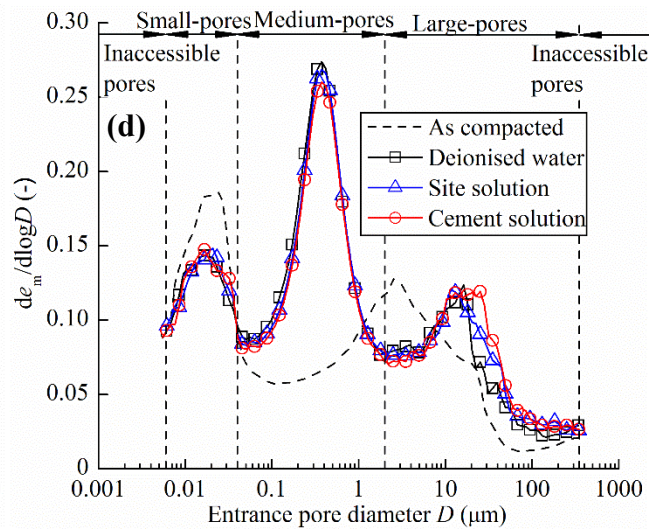
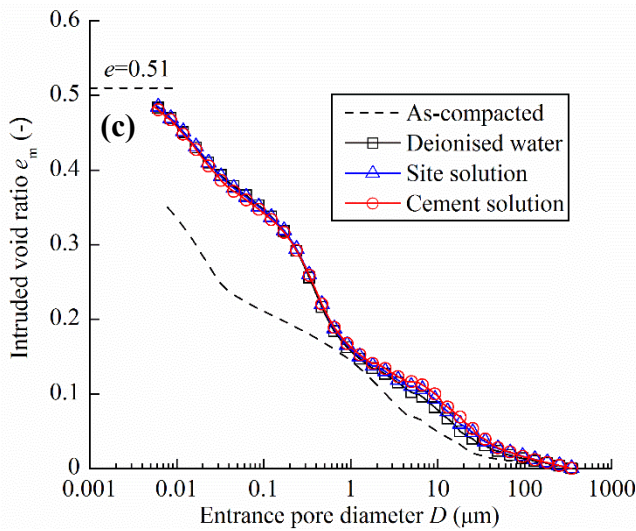
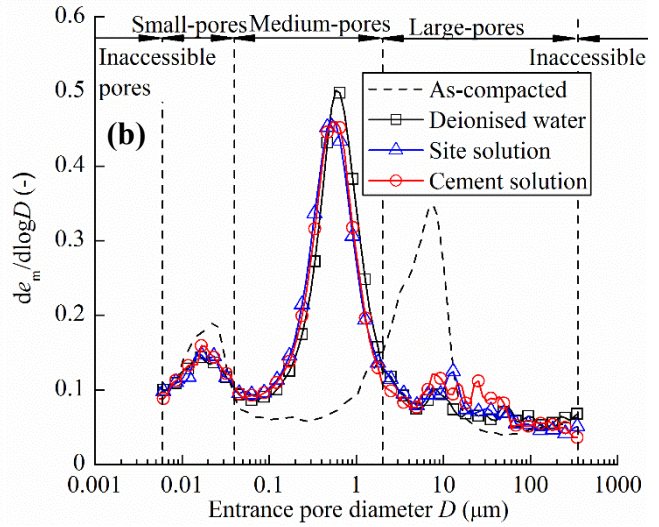
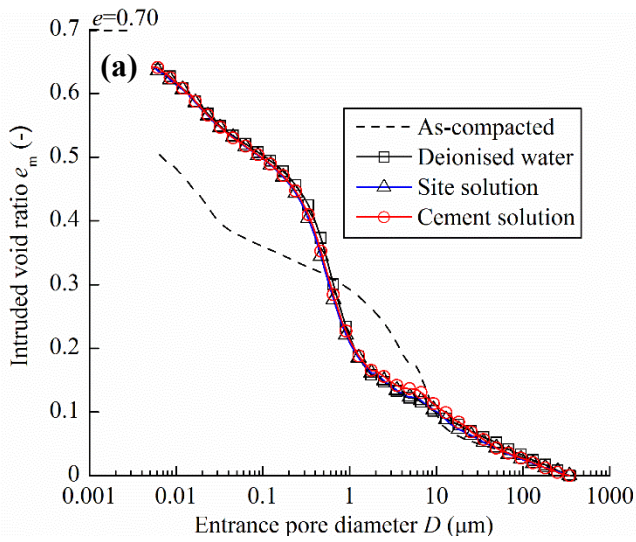
536

537

538

539

Fig. 6 Pore size distribution of MX80 bentonite/claystone mixtures: (a) cumulative curves of specimens at a dry density of 1.6 Mg/m³, (b) density function curves of specimens at a dry density of 1.6 Mg/m³, (c) cumulative curves of specimens at a dry density of 1.8 Mg/m³, (d) density function curves of specimens at a dry density of 1.8 Mg/m³, (e) cumulative curves of specimens at a dry density of 2.0 Mg/m³ and (f) density function curves of specimens at a dry density of 2.0 Mg/m³



540

541

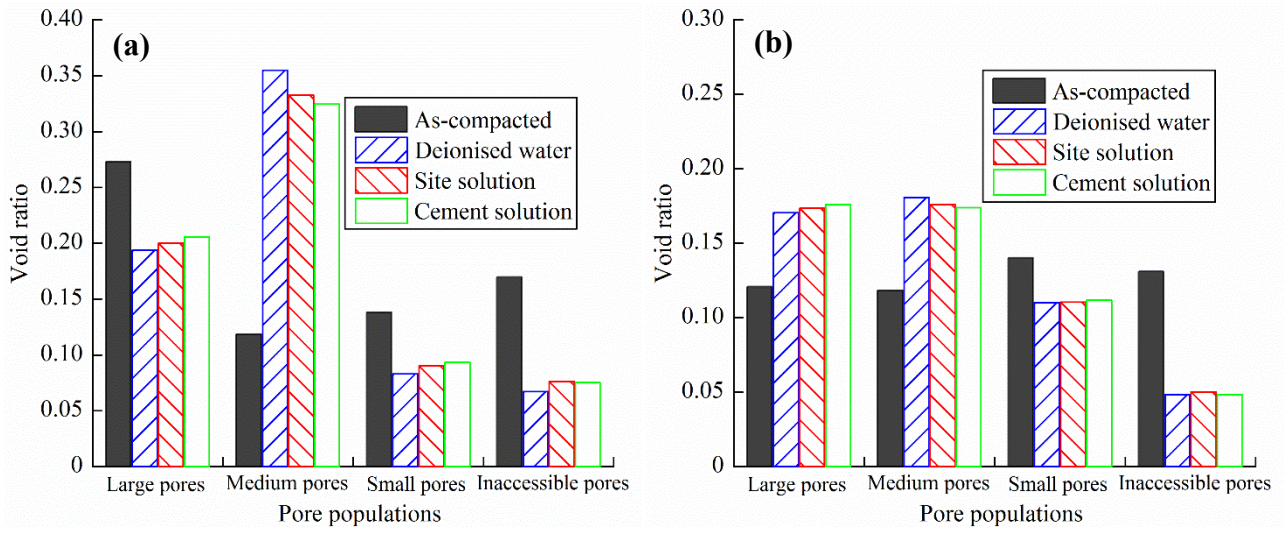
542

543

544

Fig. 7 Pore size distribution of Sardinia bentonite/claystone mixtures: (a) cumulative curves of specimens at a dry density of 1.6 Mg/m³, (b) density function curves of specimens at a dry density of 1.6 Mg/m³, (c) cumulative curves of specimens at a dry density of 1.8 Mg/m³ and (d) density function curves of specimens at a dry density of 1.8 Mg/m³

545



546

547

548

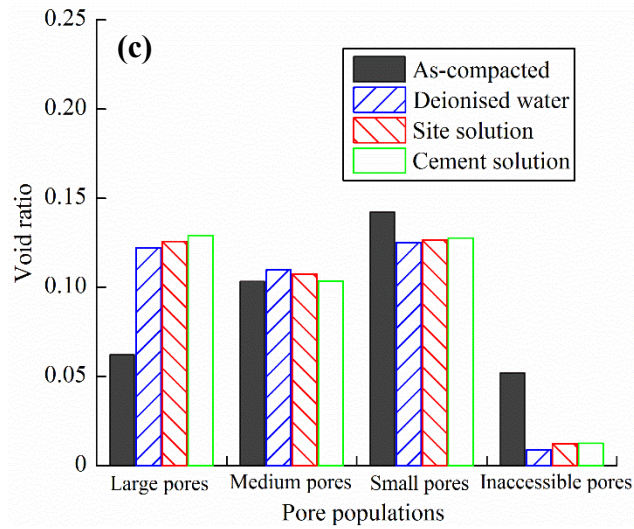


Fig. 8 Changes in inaccessible-pore, small-pore, medium-pore and large-pore void ratios for the compacted MX80 bentonite/claystone mixtures. (a) 1.6 Mg/m³, (b) 1.8 Mg/m³ and (c) 2.0 Mg/m³

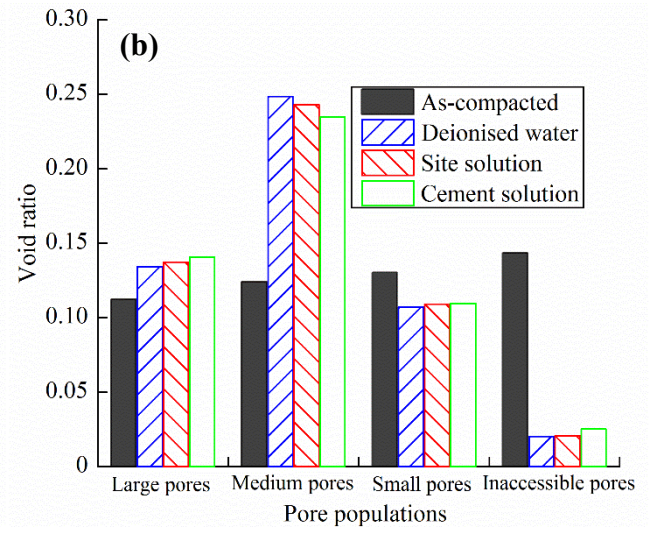
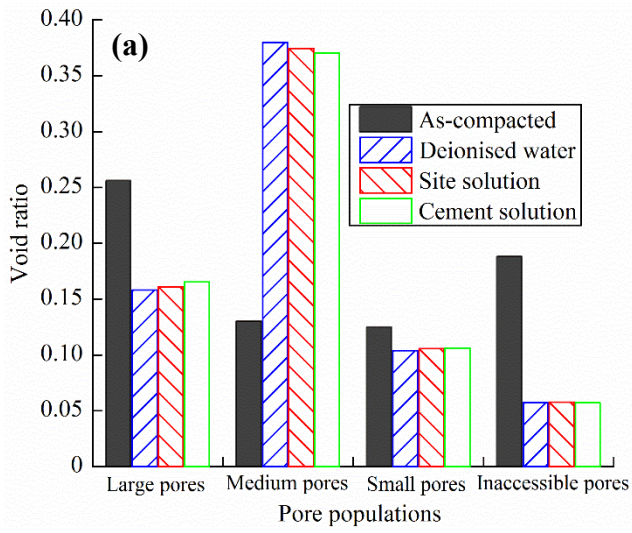


Fig. 9 Changes in inaccessible-pore, small-pore, medium-pore and large-pore void ratios for the compacted Sardinia bentonite/claystone mixtures. (a) 1.6 Mg/m³ and (b) 1.8 Mg/m³

549
550
551